Mathematical Biosciences and Engineering

MBE, 16(5): 5862–5876
DOI: 10.3934/mbe.2019293
Received: 01 March 2019
Accepted: 17 June 2019
Published: 24 June 2019

http://www.aimspress.com/journal/MBE

Research article

Biomechanical and neuromuscular strategies on backward somersault landing in artistic gymnastics: A case study

Chengliang Wu[1, 2], Weiya Hao[3,*], Wei He[3], Xiaofei Xiao[4], Xuhong Li[5] and Wei Sun[6]

[1] School of Kinesiology, Shanghai University of Sport, Shanghai, 200438, China
[2] School of Physical Education and Health, Chongqing Three Gorges University, Chongqing, 404100, China
[3] China Institute of Sport Science, Beijing, 100061, China
[4] School of Rehabilitation Medicine, Binzhou Medical University, Yantai, Shandong, 246005, China
[5] School of Physical Education and Health, Hangzhou Normal University, Hangzhou, Zhejiang, 310004, China
[6] Sports Biomechanics Lab, Shandong Institute of Sports Science, Jinan, 250002, China

* **Correspondence**: Email: haoweiya@ciss.cn; Tel.: +86-10-87182517; Fax: +86-10-87182600.

Abstract: Landing is a crucial factor in gymnastics competitions, but the underlying biomechanical and neuromuscular strategies remains unclear. This study aimed to investigate the biomechanical characteristics and neuromuscular strategies of landing for backward somersault. A 19-segment human model was developed and bilateral lower-limb joint loadings were estimated using computer stimulation. Bilateral lower-limb joint angles, vertical ground reaction force (vGRF), impulse, joint reaction force, joint torque, power, work, stiffness and electromyogram (EMG) of the rectus femoris, biceps femoris, tibialis anterior, and lateral gastrocnemius were presented during initial (touchdown to peak vGRF) and terminal impact-phases of landing (peak vGRF to vGRF equaling to body weight). The hip, knee, and ankle joints were rapidly flexed (8 º, 20 º, and 18 º, respectively) during initial impact-phase and maintained at around 90 º, 120 º, and 60 º, respectively terminal impact-phase. Flexor and extensor torques were demonstrated for lower-limb joints during initial and terminal impact-phases, respectively. The stiffness of lower limb joints and the EMGs amplitude of all examined muscles during terminal impact-phase were several times larger than that during initial impact-phase. The absolute symmetry indexes were less than 10% for lower limb joint angles and larger than 10% for the kinetics and muscle activation. The findings demonstrated symmetrical motion for lower limb joints with flexing rapidly at initial impact-phase and maintaining unchanged at terminal impact-phase and asymmetry in joint loading and muscle activation during landing.

Keywords: gymnastics; simulation; lower-limb joints; landing impact; symmetry

1. Introduction

Every event in gymnastics ends with a landing. In gymnastics competition landing is a crucial factor that affects the final result. However, previous studies indicated a meager rate of landing success in gymnastics, with an error rate as high as 71.9% on floor exercise as shown by 97 men gymnasts in 2004 [1]. Due to aesthetics, the Code of Points of the International Federation of Gymnastics (FIG) does not allow gymnasts to show ground adjustments of their feet, unsteadiness, incomplete twist, loss of balance, and fall [2]. The flexion of the lower limb joints should not be too much to keep an aesthetic and safe posture during dismount. These requirements suggest that gymnasts are trained to use a pattern of stiff landing [3], and their lower limb joints are loaded with higher loadings compared with non-gymnasts [4]. Furthermore, gymnasts are used to loading a tremendous vertical ground reaction force (vGRF) during the landing. The peak vGRF (PvGRF) of forward somersault is 7.6–15.8 body weight (BW), that of backward somersault (BS) is 7.1–13.2 BW [5]. Besides, gymnasts have a high injury risk of the lower limb in dismount [6]. A study has indicated that injuries to the lower limb during competition and practice account for 53% and 69%, respectively, of the total amount of injuries [7].

Gymnasts should perform every landing as symmetrically as possible. Asymmetrical loading increases lower extremity injury risk [8]. Sabick et al. [9] suggested that gymnasts have more symmetry in vGRF of landing than non-gymnasts, and the excellent symmetry between the legs in gymnasts is likely due to the equally distributed load among the lower limbs to decrease the risk of injury. In contrast to other sports, such as running or ball games, the dismount in gymnastics requires the execution of prescribed movement patterns and a symmetric landing [10]. Therefore, the landing strategy for the entire body and multi-joint movement used by gymnasts may be more complex than that landing in other sports. However, limited studies have used the biomechanical response of lower limbs to analyze the symmetry in the landing of gymnasts.

Landing is a complex movement under neuromuscular control, involving prediction of the space-time of the touchdown and magnitude of the vGRF. Meanwhile, the angular displacement and position of multi-joints during landing are controlled by the synergy of antagonist-agonist muscles [4]. Leg and joint stiffness of the lower limbs is the most critical regulatory factor during landing. This stiffness is modulated by appropriate muscles pre-activation prior to touchdown during landing [11]. It was reported that the average stiffness of the overall musculoskeletal system is represented by leg stiffness and the mechanics and kinematics of the body's interaction with the ground could also be affected by this stiffness [12]. However, how joint stiffness and the neuromuscular system are modulated during gymnastics landing is unclear. Furthermore, previous studies generally analyzed the whole impact phase that was defined from the initial ground contact to the maximal knee flexion [4] or the maximal descending height of body mass center [13], or the local minima in the vertical reaction force [14], and the first 100 ms [15]. However, there could be different and biomechanical and neuromuscular strategies of the lower limbs during initial and terminal impact-phases of the landing, so we attempt to quantify the kinematics, kinetics, and electromyogram (EMG) characteristics of the lower limbs during the different impact-phases. The results will help elucidate the process of gymnastics landing, energy dissipation, symmetry, and injury mechanism of the lower

limbs. Given the ethical limitations, using an *in-vivo* implanted sensor to test the internal load of the human lower limb is complicated. However, this issue could be solved by computer simulation of movements of human body. Computer simulation of the human body provides a practical approach to explore the characteristics of body motion and has been widely used to analyze body movement in humans [16].

BS is considered a fundamental skill that competitive gymnasts should a master is used very frequently in gymnastics training and competitions, and is also the basis for developing difficulty levels in movement and combined motion. This study aimed to investigate the biomechanical and neuromuscular strategies of motor control on BS landing. We hypothesized that (1) the flexion of lower limb joints is an active process at initial ground contact, and (2) the gymnast would exhibit different symmetry in kinematics, kinetics, and EMGs recordings between the left and right legs during the landing.

2. Materials and method

2.1. Participant

The participant was an international-level gymnast from the Chinese national team competing in World Cups and Championships (male, mass: 63 kg, age: 17 years), and with no musculoskeletal injuries for at least 6 months prior. A total of 31 individual anthropometric parameters, such as standing height and waist depth, were measured (Table 1). The gymnast read and provided signed informed consent, and the study conformed to the protocol of the Ethical Advisory Committee of China Institute of Sport Science (CISS).

Table 1. Anthropometric measurement data (cm).

Measurements	Value	Measurements	Value	Measurements	Value
Standing height	168	Chest breadth	32	Waist circumference	17
Shoulder height	137	Waist depth	19	Knee height seated	45
Armpit height	125	Waist breadth	26	Thigh circumference	55
Waist height	93	Buttock depth	23	Upper leg circumference	41
Seated height	60	Hip breadth standing	31	Knee circumference	37
Head length	19	Shoulder to elbow length	32	Calf circumference	38
Head breadth	16	Forearm–hand length	29	Ankle circumference	23
Head to chin height	25	Biceps circumference	32	Ankle height, outside	9
Neck circumference	39	Elbow circumference	29	Foot breadth	9
Shoulder breadth	38	Forearm circumference	28	Foot length	24
Chest depth	21				

2.2. Instrumentation

Kinematic data were collected with a 9-camera Qualisys Oqus motion capture system at 250 Hz. Retro reflective markers (16 mm diameter) were placed at the head, cervical vertebrae (CV7), scapula-inferior angle, thoracic vertebrae (TV10), shoulder, elbow, wrist, anterior superior iliac spine, posterior superior iliac spine, knee, ankle, metatarsal-phalangeal joints, heel, and toes on both sides

of the body (Figure 1), the place of these markers were referenced from the CAST full body marker set [17]. A Kistler force plate located beneath a landing mat (5 cm thick), which has little influence on the research since it has been reported that there is less than 5% difference in GRF when the thickness is up to 12 cm thick [14], was used to collect GRF data (1000 Hz), and the surrounding floor was an ethylene-vinyl acetate insole mat. Muscle activation patterns were recorded (surface EMGs, 2000 Hz), with a gain of 3000, from the rectus femoris (RF), biceps femoris (BF), tibialis anterior (TA), and lateral gastrocnemius (LG) on the two lower limbs of the gymnast using a portable DELSYS Trigno^{TM} wireless EMGs system, the place of these EMG sensors were referenced from the SENIAM guidelines [18]. The EMG sensors were fixed on the skin using specialized double-sided tape and medical tape. The Qualisys Oqus motion capture system, the force plate, and the surface EMGs system were all synchronized using a radio signal (Figure 2).

2.3. Procedures

Data collection was conducted in the laboratory of CISS. The gymnast initially performed a warm-up exercise (15 min of jogging, skipping, and stretching). Subsequently, the markers and surface electrodes were placed. The gymnast performed three trials of BS without taking a step or hop. The BS was initiated by jumping from the ground next to the force plate with bare feet, and the best trial was qualitatively judged by two national-level coaches using the Code of Points of the FIG. Meanwhile, the 3D motion data, EMGs, and vGRF data were simultaneously being recorded separately by the Qualisys Oqus motion capture system, the surface EMGs system, and the force plate respectively.

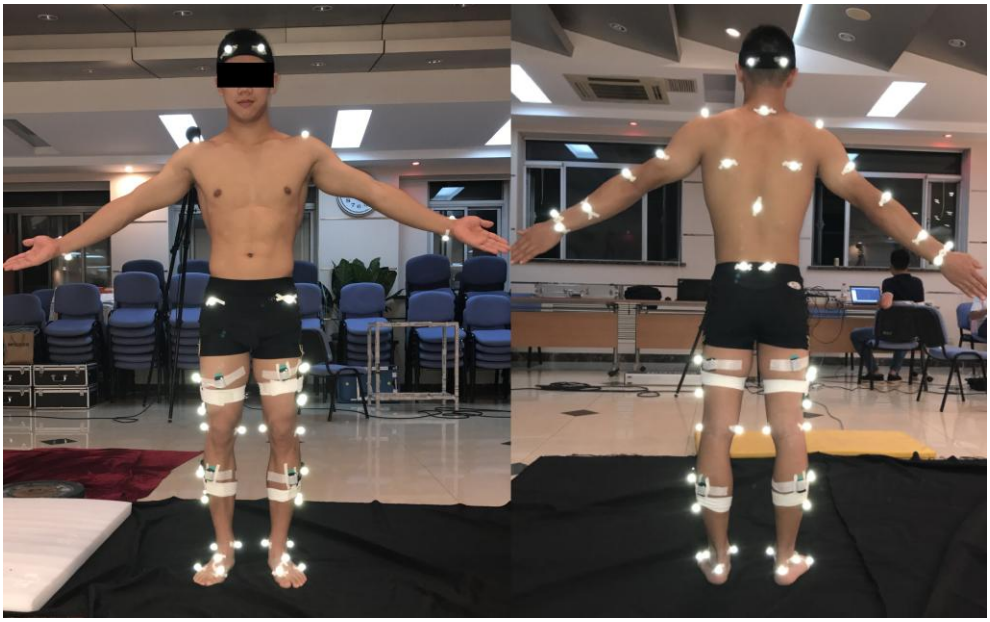

Figure 1. Location of retro-reflective markers and EMG sensors on the gymnast. The wireless EMG sensors were positioned on the rectus femoris (RF), biceps femoris (BF), tibialis anterior (TA), and lateral gastrocnemius (LG) of the lower limbs. These sensors were secured with specialized double-sided tape and medical tape. Positions of these markers and sensors were referenced from the CAST full body marker set [17] and the SENIAM guidelines [18], respectively.

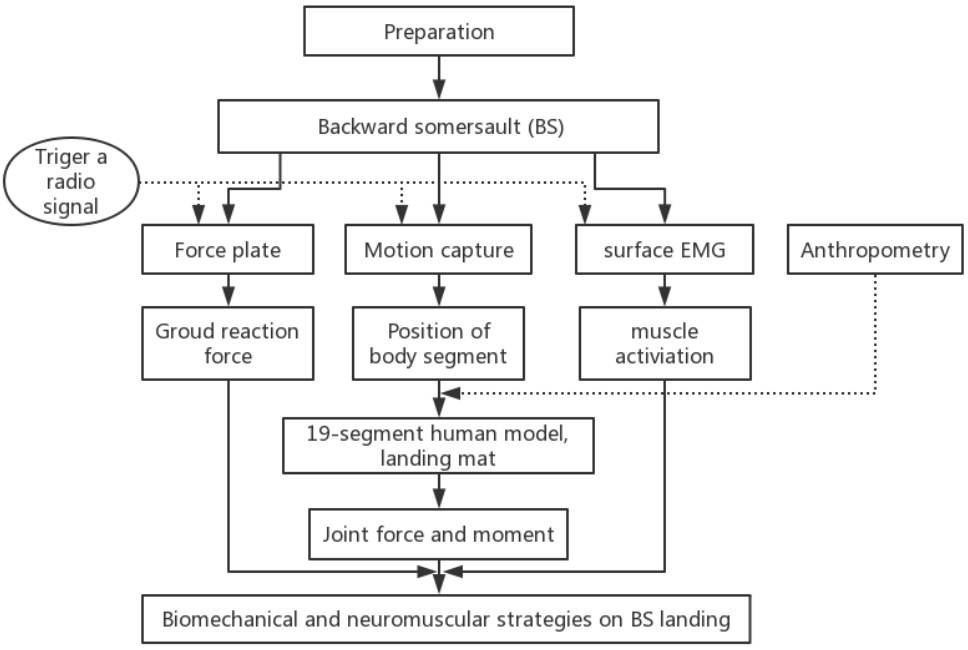

Figure 2. The diagram of data collection with synchronization. The gymnast performed backward somersault landing after warm-up exercise. Meanwhile, the markers trajectories, ground reaction forces, and EMGs of the gymnast were synchronously recorded using a radio signal. After that, joint forces and moment were calculated using a human multi-body model for analyzing biomechanical and neuromuscular strategies.

2.4. Biomechanical modeling and simulations

The GeBod (Generator of Body Data) database (BRG.LifeMOD^{TM}) was used to develop a 19-segment rigid-body model based on age, mass, and personalized anthropometric data of the gymnast (Table 1). The measurement parameters used in GeBod are detailed by Cheng et al. [19]. These anthropometrics measures were used to generate a personalized model. The model consisted of the head, neck, upper torso, central torso, lower torso, scapulas, upper arms, lower arms, hands, upper legs, lower legs, feet, and 18 human joints [20], and computer simulation was performed using the landing 3D motion data. A model of gymnastics matting with a dimension of 2 × 2 × 0.05 m (length × width × height) was developed using the MSC.ADAMS (MSC Software Corp. acronym of Automated Dynamic Analysis of Mechanical Systems) software. The base of the mechanical properties of the landing mat was obtained by an optimization algorithm (equations (1) and (2)) [21].

$$\Delta\delta = \sqrt{\frac{(x_1 - y_1)^2 + (x_2 - y_2)^2 + \ldots + (x_n - y_n)^2}{n}} \tag{1}$$

$$S = [\Delta T + \Delta vGRF + \frac{1}{3}\sum \Delta Jo\,\text{int}\,angles] \tag{2}$$

where x_i is the kinematic data from real performance, y_i is the kinematic data from computer simulation, and $\Delta\delta$ is RMS (root mean square) error between real performance and

simulation; ΔT is expressed as RMS error of time to peak vGRF; $\Delta vGRF$ is expressed as RMS error of vertical ground reaction forces; $\Delta Joint\ angles$ is expressed as RMS error of joint angles of lower limbs; and n is the number of data points with each curve; the best optimal parameters are determined when S is the minimum.

The model was validated by the curve of the dynamic changes (equation (3)) [21].

$$CMC = \sqrt{1 - \frac{\sum_{i=1}^{m}\sum_{j=1}^{n}(x_{ij} - \bar{x}_j)^2 / n(m-1)}{\sum_{i=1}^{m}\sum_{j=1}^{n}(x_{ij} - \bar{x})^2 / (nm-1)}} \quad (3)$$

where m is the number of all curves, n is the number of data in each curve, x_{ij} is expressed as the j-th data of the i-th curve, $\bar{x}_j$ is the average of the j -th data of all curves, and $\bar{x}$ is the overall average of data of all curves. To examine the reliability of the model, coefficients of multiple correlation (CMC) between the simulation and actual results from the participant were calculated, with 0.25–0.50, 0.50–0.75, and >0.75, indicating poor, moderate, and good correlations, respectively [22]. The actual results were recorded during the real performance of the gymnast using the motion capture and force plate, including joint angles of the lower limbs and vGRF.

2.5. Data analysis

Landing impact phase was defined from the touchdown to vGRF equaling to BW, which is after PvGRF. The touchdown was identified as the first frame when vGRF exceeded 10 N [4] on professional software (BioWare, Kistler Instrument Ltd., Switzerland). Meanwhile, the impact phase was divided into two phases (T1: initial impact-phase, from the first touchdown to the PvGRF; T2: terminal impact-phase, from the PvGRF to the vGRF equaling to BW). The joint angles were calculated between two lines in space base on three trajectories, and selected the trajectories that we want to match with the markers. The data for PvGRF was normalized based on the body weight of the gymnast, and impulse of a force was calculated as the integral of the vGRF over its period of application. Power approach was used to determine joint work by quantifying joint velocities (angular) and joint kinetics (torque). Support moment (M_s) is the total extensor pattern at all three joints of the lower limb [23]. Raw EMGs signals were full-wave rectified, and band-pass filtered with a Butterworth filter with cut off frequencies at 10–400 Hz [24]. Pre-activation phase was determined as 100 ms preceding touchdown [25]. The root mean square of EMGs (EMG_{RMS}) was calculated in the pre-activated (T0) and two impact phases of landing (T1 and T2) (equation (4)). The EMGs signals were normalized by peak EMG in the landing phase. In each sub-phase, antagonist–agonist coactivation was calculated as the TA to LG normalized EMGs for the ankle, and the BF to RF normalized EMGs for the knee [26].

$$\mathrm{RMS}[EMG(t)] = \sqrt{\frac{1}{\mathrm{T}}\int_{t}^{\mathrm{t+T}} \mathrm{EMG}^2\,(\mathrm{t}) \cdot \mathrm{dt}} \quad (4)$$

where EMG is the value of the EMG signal at each moment of time (t), and T represents the duration of the analyzed signal.

The absolute symmetry index (ASI) was used to calculate the symmetry between the feet

(equation (5)).

$$\text{ASI} = \left|\frac{(x_l - x_r)\times 2}{(x_l + x_r)}\right| \times 100\% \quad (5)$$

where x_l and x_r are the values of the landing variable for the left and right foot, respectively. When ASI = 0, the landing is symmetrical. ASI of less than 10% is an acceptable degree of symmetry [27].

The angles of the two lower limb joints were recorded on the sagittal-plane during the landing. These joint torques were calculated with computer simulation using the software based on the lagrangian formalism [23]. To calculate joint stiffness, the following equation (6) was used:

$$\text{Joint stiffness} = {}^{\Delta M}/_{\Delta\theta} \quad (6)$$

where ΔM is the change of the joint torque, and $\Delta\theta$ is the angular displacement of the joint flexion [4].

3. Results

3.1. Kinematics of landing

The lower limb joints flexed considerably rapidly, and flexions of the hip, knee, and ankle (dorsiflexion) changed by 8 °, 20 °, and 18 °, respectively, on average during T1 (Figure 3). However, the flexion of these joints maintained at around 90 º, 120 º, and 60 º, respectively, during T2 (Figure 3). The ASIs of flexion of these joints were less than 10% (except the ankle during T2, 10.2%). The flexion of the hips, knees, and ankles by simulation correlated well to the actual measured results in the angles of left knee (CMC = 0.95), right knee (CMC = 0.93), and left and right ankles (CMC = 0.85).

3.2. Kinetics of landing

The CMC of the simulated and actual measured vGRF was 0.86, and the measured PvGRF was 12.5 BW. The difference between the measured and simulated PvGRF (11.9 BW) was 4.6%, and the time for the simulated and measured vGRFs to reach a peak differed by 6 ms (Figure 4a). The simulated PvGRFs of the left and right feet were 3614 N and 3610 N, respectively. The impulse of vGRF was shaped like an S curve (Figure 4b), and the impulse increment was the fastest before and after the PvGRF. The joint reaction force (JRF) of the ankles, knees, and hips rapidly increased during T1 (Figure 4c, Figure 4b). In comparison to the PvGRF, peak JRFs of the left ankle, knee, and hip were delayed by 6, 10, and 20 ms, with a delay of 14, 18, and 26 ms for the right side, respectively. The peak JRFs were not reached until T2. Furthermore, hips and knees were loaded by the flexor torque during T1 and by the extensor torque during T2 (Figure 5). The power and work of the hips and knees were considerably altered during T1, and the power and work increment of the joints tended to be relatively stable during T2 (Figure 6). Besides, the increment in the joint stiffness of the hips, knees, and ankles were 2.3, 12.3 and 7.3-fold, respectively, from T1 to T2 (Table 2). Besides, the ASIs of the kinetics (including vGRF, JRF, torque, power, work and stiffness) of the lower limb joints were all more than 10% (Table 3).

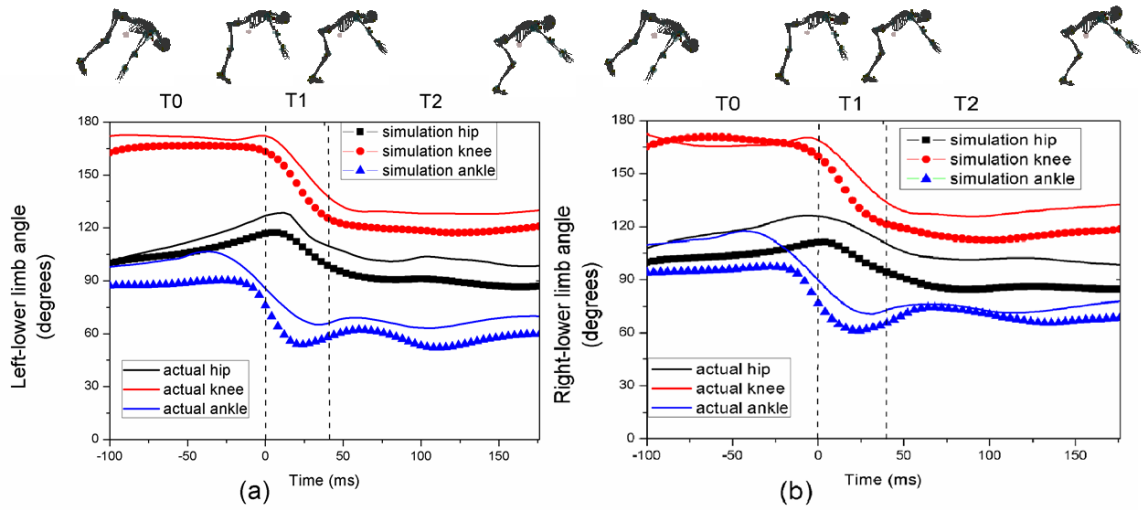

Figure 3. Joint angles in the sagittal plane during the simulation and actual landing. (a: left leg; b: right leg). The skeleton models showed four body postures of the landing (100 ms prior touchdown, touchdown, peak vertical ground reaction force (vGRF), and vGRF equal to body weight, respectively). (The whole landing process was divided into three phases by dotted lines. T0: The pre-activation phase was defined as 100 ms preceding touchdown; T1: initial impact-phase, from the first touchdown to the peak vGRF; T2: terminal impact-phase, from the peak vGRF to the vGRF equaling to body weight).

Table 3. Absolute symmetry index (ASI) of the lower limbs during the initial impact-phase (T 1) and terminal impact-phase (T 2). (Mean %)

	hip		**knee**		**ankle**		**foot**	
	T1	**T2**	**T1**	**T2**	**T1**	**T2**	**T1**	**T2**
Kinematics								
Joint angles	2.3	0.6	3.2	1.9	4.5	10.2		
Kinetics								
vertical GRF							21.1	42.5
Joint reaction force	17.7	59.4	26.0	52.8	33.3	48.5		
Joint torque	70.4	82.5	42.0	51.7	39.1	27.2		
Power	99.0	148.3	50.7	259.3	129.3	201.3		
Work	101.8	109.6	62.5	54.1	33.3	47.4		
Joint stiffness	23.0	39.7	60.1	23.8	49.8	12.4		
Electromyography								
Coactivation			157.5	11.0	32.7	57.4		

T1: initial impact-phase, from the first touchdown to the peak vertical ground reaction force (vGRF); T2: terminal impact-phase, from the peak vGRF to the vGRF equaling to body weight (BW).

Table 2. Joint stiffness of the hip, knee, and ankle in the initial impact-phase (T_1) and terminal impact-phase (T_2). (Nm/kg deg^{-1})

	Left hip	Left knee	Left ankle	Right hip	Right knee	Right ankle
T1	0.18	0.06	0.01	0.14	0.03	0.02
T2	0.41	0.46	0.13	0.61	0.58	0.12

T1: initial impact-phase, from the first touchdown to the peak vertical ground reaction force (vGRF); T2: terminal impact-phase, from the peak vGRF to the vGRF equaling to body weight (BW).

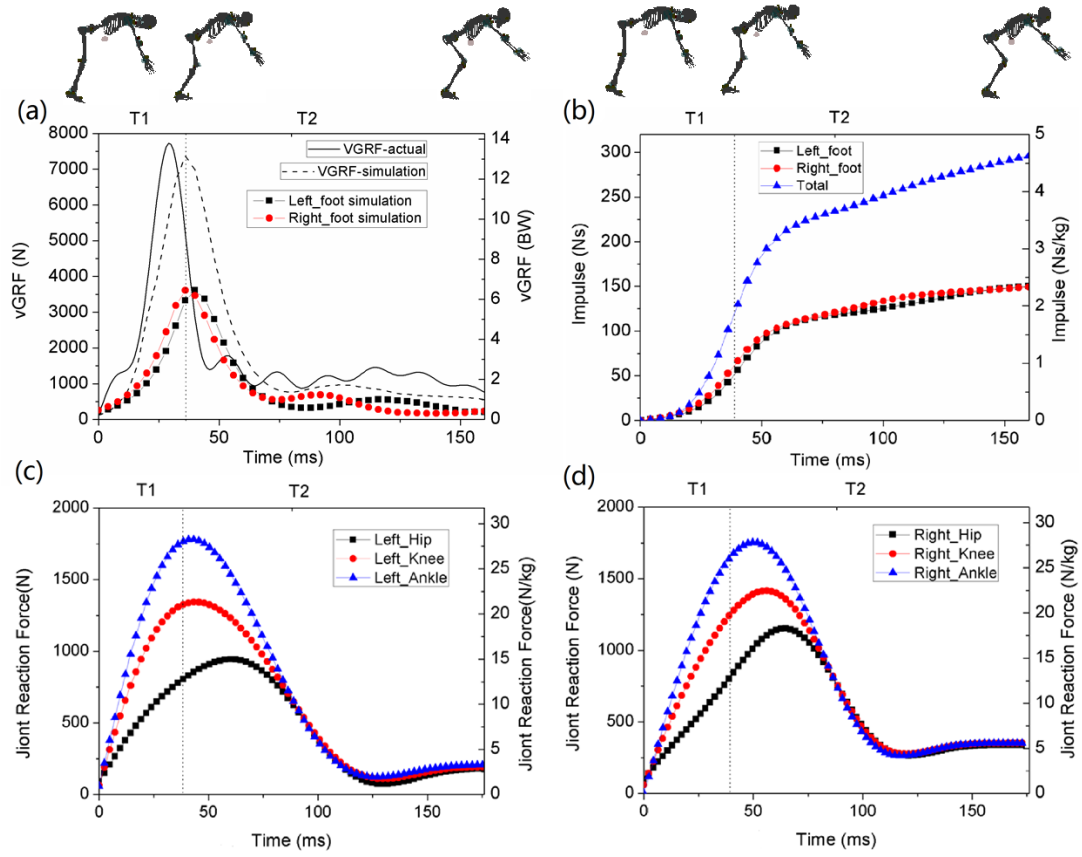

Figure 4. The measured vertical ground reaction force (vGRF) and the simulated results during the landing (a). Impulse of vGRF (b). Joint reaction force at the lower limbs (c: left leg; d: right leg) during the landing. The skeleton models showed three body postures of the landing (touchdown, peak vGRF, and vGRF equal to body weight, respectively). (The impact phase of landing was divided into two phases by dotted line. T1: initial impact-phase, from the first touchdown to the peak vGRF; T2: terminal impact-phase, from the peak vGRF to the vGRF equaling to body weight).

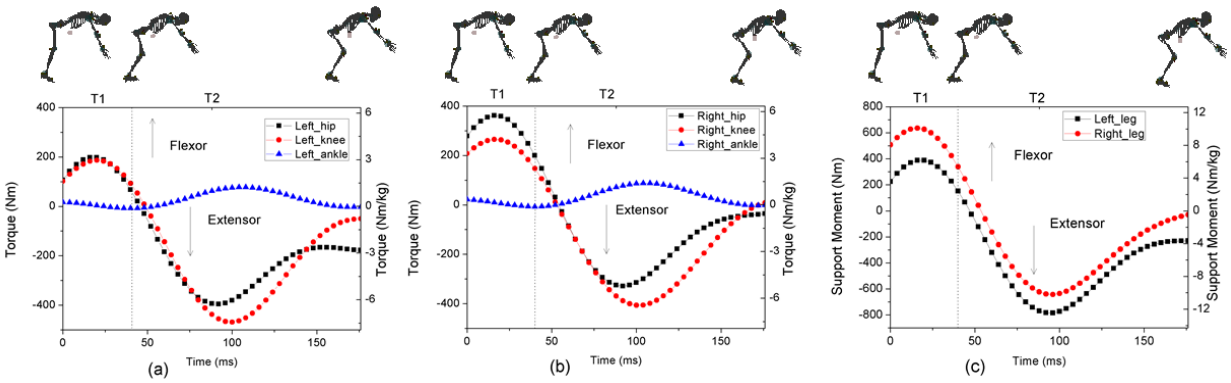

Figure 5. Joint torque at the lower limbs in sagittal plane. Positive values indicate flexor or plantarflexor torque (arrow up), and negative values indicate extensor or dorsiflex torque (arrow down). The support moment (M_s) is the total extensor pattern at all three joints. $M_s = M_{hip} + M_{knee} + M_{ankle}$. The skeleton models showed three body postures of the landing (touchdown, peak vertical ground reaction force (vGRF), and vGRF equal to body weight, respectively). (The impact phase of landing was divided into two phases by dotted line. T1: initial impact-phase, from the first touchdown to the peak vGRF; T2: terminal impact-phase, from the peak vGRF to the vGRF equaling to body weight).

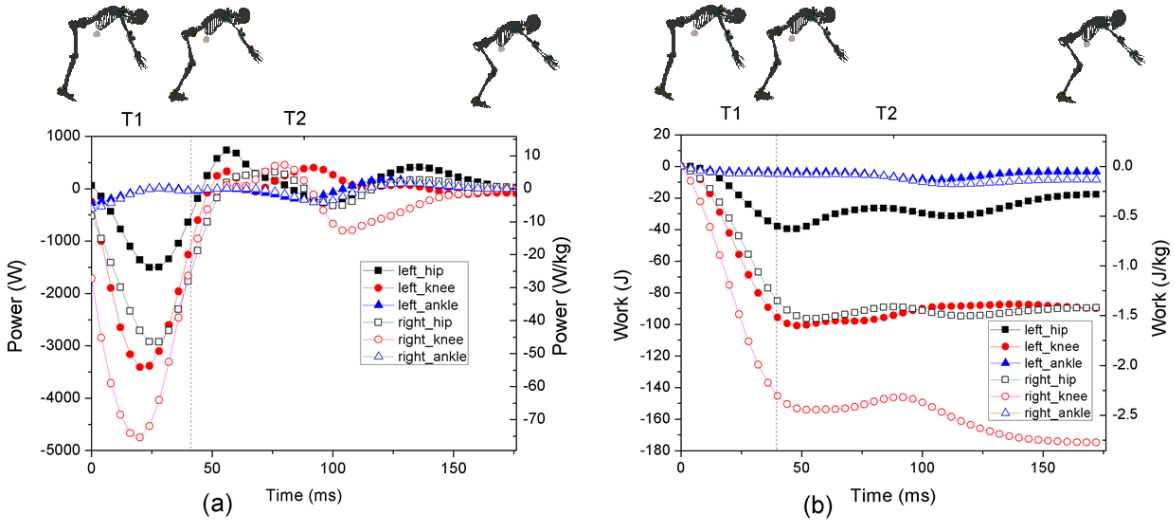

Figure 6. Power (a) and work (b) of the lower limbs. Positive and negative values indicate energy generation (concentric muscle action) and energy absorption (eccentric muscle action), respectively. The skeleton models showed three body postures of the landing (touchdown, peak vertical ground reaction force (vGRF), and vGRF equal to body weight, respectively). (The impact phase of landing was divided into two phases by dotted lines. T1: initial impact-phase, from the first touchdown to the peak vGRF; T2: terminal impact-phase, from the peak vGRF to the vGRF equaling to body weight).

3.3. Electromyography

The EMGs of all examined muscles (RF, BF, TA, and LG of the both lower limbs) were activated during T0, and the peak EMGs were all in T2 (Figure 7a), except that of the TA of the left leg. Furthermore, the EMG_{RMS} approximately showed an elevating trend from T0 to T2 and increased dramatically during T2 (average 4.8-fold larger than that during T1) (Figure 7b). More specifically, the coactivation of the knees and ankles all ranged between 0.76 and 1.38 during T2, which involved the highest activation level, and their ASIs were more than 10% during T1 and T2 (Table 3).

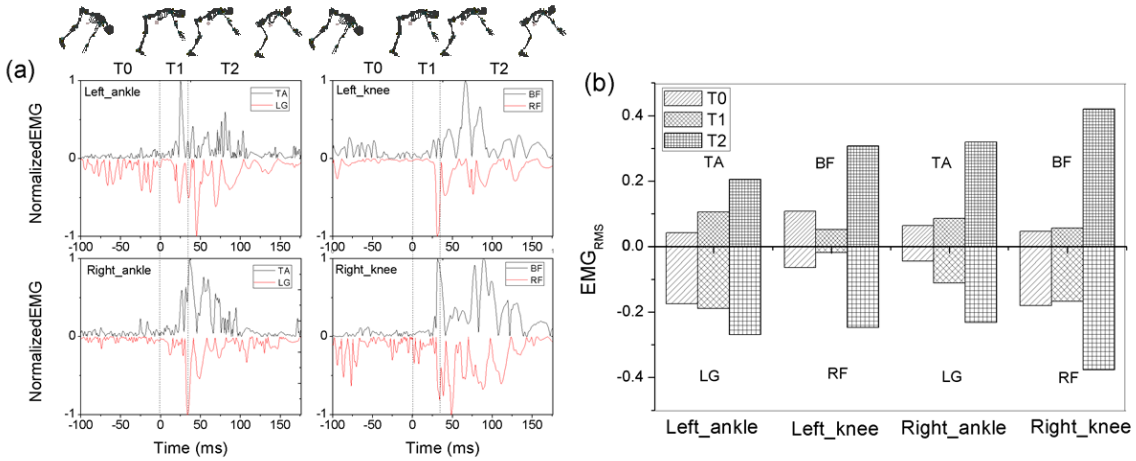

Figure 7. Coactivation of normalized EMGs (a) and root mean square of normalized EMG (EMG_{RMS}) (b). Positive EMG/EMG_{RMS} means antagonist of the joint, and negative EMG/EMG_{RMS} means the agonist of the joint. The EMGs were normalized to the peak EMG during the landing phase. The coactivation was defined as the TA to LG EMGs for the ankle, and the BF to RF EMGs for the knee. (RF: rectus femoris, BF: biceps femoris, TA: tibialis anterior, LG: lateral gastrocnemius). The skeleton models showed four body postures of the landing (100 ms prior touchdown, touchdown, peak vertical ground reaction force (vGRF), and vGRF equal to body weight, respectively). (The whole landing process was separated into three phases by dotted lines. T0: The pre-activation phase was defined as 100 ms preceding touchdown; T1: initial impact-phase, from the first touchdown to the peak vGRF; T2: terminal impact-phase, from the peak vGRF to the vGRF equaling to body weight).

4. Discussion

This work is the first to comprehensively investigate the biomechanical and neuromuscular strategies during BS landing performed by an international level gymnast during initial (T1) and terminal (T2) impact-phase. The lower limb joints showed flexor torque in T1 and extensor torque in T2; during T2, the JRFs, joint torques, joint stiffness, and EMGs were higher than those in T1, but the flexions of the lower limb joints in T2 were less. Furthermore, these flexions showed symmetry between the left and right legs during the landing, but the kinetics and EMGs data were asymmetrical.

The model successfully reproduced the joint angles and kinetics characteristic of the BS landing. The measured flexion of the lower limb joints and vGRF were close to the simulation results. The CMCs presented high correlation (>0.75). Furthermore, the difference between the simulated (11.9 BW) and measured PvGRF (12.5 BW) was 4.6%. The PvGRF was consistent with that of previous studies (7.1–13.2 BW) [5]. Therefore, the results suggested the human model was valid.

Neuromuscular pre-activation plays a significant role in the landing strategy. The RF, BF, LG, and TA of the lower limbs were activated during T0. Previous studies also showed that the LG, TA, and vastus lateralis of gymnasts were all in the pre-activated phase before touchdown and that the activation level of gymnasts was higher than that of non-gymnasts [4].

As hypothesized, the landing strategy of the gymnast was to actively flex his lower limb joints in the initial impact-phase (T1). Flexion and flexor torques of the hips, knees, and ankles rapidly increased during T1. The lower limb joints were suggested to actively flex to absorb considerable kinetic energy. An appropriate lower limb joint angle during the dismount of touchdown raises the ability of the muscles to absorb energy [28]. In this study, the time to PvGRF was 30 ms, which was close to that in our previous results [21]. The energy during landing can be absorbed by athletes through flexion motion of the lower limb joints [15]. More impact energy could also be dissipated with greater flexion angle of the lower limb joints [3,5]. However, the flexion angle of these joints should be minimized during landing because of the restriction of gymnastic regulations [2]. Thus, energy dissipation was probably limited during T1 for the gymnast.

The landing strategy of the gymnast was to dissipate the landing impact, controlling the flexion movements of the lower limbs in a small range during the terminal impact-phase (T2). The angle of the lower limb joints changed by a lesser amount, indicating that the body tended to stabilize. T2 took a relatively long time (approximately five times of T1), but increment in the impulses of the lower limb was less than one-third of that in T1, thus the landing impact was well dissipated. Furthermore, the JRF of the ankles, knees, and hips rapidly increased during T1, but their peaks were reached during T2. This result indicates the delay effect of the JRF by 14-26 ms after PvGRF and that the conduction of vGRF to the human body was a gradual process from the ankle to the knee and then to the hip. Therefore, the force was successively reduced, and dissipating of the landing impact was realized by the excellent coordination of the three lower limb joints to adequately protect the trunk and cephalic organs [29]. Moreover, the support moment is the total extensor pattern at all three joints, and therefore it contributes to defending against the landing-induced body collapse [23]. The eccentric work of the knee joint was maximum, followed by the hip and ankle joints, which was consistent with the overall trend of the results during the drop landing in previous studies [6]. On the other hand, the stiffness and EMG_{RMS} of both the lower limb joints increased several times from T1 to T2. Therefore, the co-contraction could increase joint stiffness, thereby limiting the flexion of the lower limb joints to achieve more stable gymnastic landing performance. Park and Durand [30] suggested that joint stiffness is nearly controlled by the level of muscle co-contraction. The ankle needed to bear the maximum impact load, but lack of effective energy dissipation due to minimum flexion angle and eccentric work. Therefore, we speculated that the risk of injury of the ankle was probably the highest during gymnastic landing among the lower limb joints, which was consistent with the findings of an epidemiological investigation [29].

The gymnast exhibited a different symmetry in kinematics, kinetics, and EMGs between the left and right legs during the landing. During the entire impact phase of the landing (T1 and T2), the difference between flexions of both hip and knee joints was within 5 °, and the difference in ankle

dorsiflexion was within 10 °. Furthermore, the ASIs of flexion of the lower limb joints were less than 10%. These results showed an excellent landing symmetry in sports performance. However, the ASIs of the kinetics (including vGRF, JRF, torque, power, work and stiffness) and EMGs (coactivation) of the lower limb joints were all more than 10%. The ASI of the power of ankle was even more than 200% in T2. Sabick et al. [9] speculated that a good landing symmetry between the legs in gymnasts is likely due to the equal distribution of load among the lower limbs. However, similar results were not noted in this study. This could be an indication that the internal load of the lower limb joints can efficiently modulate the landing symmetry. Van Emmerik et al. [31] suggested that the human dynamic system plays a regulatory role in the completion of movement. The change in multiple joint forces can affect the athletes' kinematic performance during sprints [32]. Therefore, a symmetrical landing could be better performed by modulating the kinetics and EMGs of the lower limbs, including vGRF, JRF, torque, stiffness, power, and eccentric work of multi-joints, and synergy of antagonist and agonist muscles.

This study had two main limitations. First, the computer simulation model was a multi-rigid body without considering the shock of soft tissues. Second, only one participant was included in the study, but the landing was comprehensively analyzed using kinematic, kinetic, and EMGs data from the international-level gymnast during initial and terminal impact-phases, these characteristics that is one of the representatives of excellent gymnastic landings. Nonetheless, most results of the model were in line with those obtained in experimental studies. Detailed musculoskeletal models may enhance our understanding of the loadings of the lower limb joints, particularly related to soft tissues. Future studies might focus on how more gymnasts manage their landing motion to ensure symmetry.

5. Conclusion

An international-level gymnast employs complex biomechanical and neuromuscular landing strategies to perform BS successfully. The relevant lower limb muscles initially pre-activate before touchdown to adequately prepare for landing. Subsequently, the gymnast actively flexes the lower limb joints at initial ground contact and then struggles to extend the joints to dissipate the landing impact and maintain an unchanged posture. Meanwhile, the gymnast may modulate lower limb joints loading and muscle activation of both the lower limbs to achieve landing symmetry. The findings of this study may expand our knowledge about gymnastics landing.

Acknowledgments

This study was supported by the National Key R&D Program of China (No. 2017YFC0803802), the National Natural Science Foundation of China (No. 11672080, 31700815), and the Chongqing Natural Science Foundation of China under Grant (No. cstc2018jcyjAX0086). The authors are thankful to the Chinese national gymnastics team for their valuable collaboration.

Conflict of interest

This manuscript has not been published or presented elsewhere in part or in entirety and is not under consideration by another journal. All authors have read and approve the content of the manuscript. The study participant provided informed consent, and the study design was approved by

the appropriate ethics review board. We have read and understood your journal's policies, and we believe that neither the manuscript nor the study violates any of these. There are no conflicts of interest to declare.

References

1. M. Marinšek and I. Čuk, Landing errors in the men's floor exercise are caused by flight characteristics, *Biol. Sport*, **27**(2010), 123–128.
2. FIG, Code of points men's artistic gymnastics. Lyss: Federation International Gymnastics, 2017.
3. I. Čuk and M. Marinšek, Landing quality in artistic gymnastics is related to landing symmetry, *Biol. Sport*, **30**(2013), 29–33.
4. A. Christoforidou, D. A. Patikas, E. Bassa, et al., Landing from different heights: biomechanical and neuromuscular strategies in trained gymnasts and untrained prepubescent girls, *J. Electromyogr. Kines.*, **32**(2017), 1–8.
5. A. Slater, A. Campbell, A. Smith, et al., Greater lower limb flexion in gymnastic landings is associated with reduced landing force: a repeated measures study, *Sports Biomech.*, **14**(2015), 45–56.
6. S. N. Zhang, B. T. Bates and J. S. Dufek, Contributions of lower extremity joints to energy dissipation during landings, *Med. Sci. Sport Exer.*, **32**(2000), 812–817.
7. S. W. Marshall, T. Covassin, R. Dick, et al., Descriptive epidemiology of collegiate women's gymnastics injuries: National collegiate athletic association injury surveillance system, *J. Athl. Training*, **42**(2007), 234–240.
8. S. Eagle, C. Connaboy, Q. Mi, et al., Asymmetrical landing patterns combined with heavier body mass increases lower extremity injury risk in special operations forces, *J. Sci. Med. Sport*, **20**(2017), S47–S49.
9. M. B. Sabick, R. K. Goetz, S. M. Kuhlman, et al., Symmetry in ground reaction forces during landing in gymnasts and non-gymnasts, *Med. Sci. Sport Exer.*, **38**(2006), S23.
10. M. J. R. Gittoes, G. Irwin, D. R. Mullineaux, et al., Whole-body and multi-joint kinematic control strategy variability during backward rotating dismounts from beam, *J. Sport Sci.*, **29**(2011), 1051–1058.
11. A. Kramer, R. Ritzmann, M. Gruber, et al., Leg stiffness can be maintained during reactive hopping despite modified acceleration conditions, *J. Biomech.*, **45**(2012), 1816–1822.
12. C. T. Farley and D. C. Morgenroth, Leg stiffness primarily depends on ankle stiffness during human hopping, *J. Biomech.*, **32**(1999), 267–273.
13. M. J. R. Gittoes, G. Irwin and D. G. Kerwin, Kinematic landing strategy transference in backward rotating gymnastic dismounts, *J. Appl. Biomech.*, **29**(2013), 235–260.
14. J. L. McNitt-Gray, D. M. E. Hester, W. Mathiyakom, et al., Mechanical demand and multijoint control during landing depend on orientation of the body segments relative to the reaction force, *J. Biomech.*, **34**(2001), 1471–1482.
15. M. J. Decker, M. R. Torry, D. J. Wyland, et al., Gender differences in lower extremity kinematics, kinetics and energy absorption during landing, *Clin. Biomech.*, **18**(2003), 662–669.
16. M. G. Pandy, Computer modeling and simulation of human movement, *Annu. Rev Biomed Eng.*, **3**(2001), 245–273.

17. J. S. V. Sint, Color atlas of skeletal landmark definitions, Guidelines for reproducible manual and virtual palpations, Edinburgh: Churchill Livingstone, (2007), 29–175.
18. H. Hermens, B. Freriks, R. Merletti, et al., European recommendations for surface electromyography, The Netherlands: Roessingh Research and Development, (1999), pp. 43–45.
19. H. Cheng, L. Obergfell and A. Rizer, The development of the GEBOD program, in *Proceedings of the 15th Southern Biomedical Engineering Conference*, Dayton, Ohio, (1996), 251–254.
20. S. Serveto, S. Barré, J. M. Kobus, et al., A three-dimensional model of the boat-oars-rower system using ADAMS and LifeMOD commercial software, *PI Mech. Eng. P-J Spo.*, **224**(2010), 75–88.
21. X. Xiao, W. Hao, X. Li, et al., The influence of landing mat composition on ankle injury risk during a gymnastic landing: a biomechanical quantification, *Acta Bioeng. Biomech.*, **19**(2017), 105–113.
22. T. D. Collins, S. N. Ghoussayni, D. J. Ewins, et al., A six degrees-of-freedom marker set for gait analysis: repeatability and comparison with a modified Helen Hayes set, *Gait Posture*, **30**(2009), 173–180.
23. D. A. Winter, Biomechanics and motor control of human movement, 4th edition, New Jersey: John Wiley & Sons, Inc., (2009), 124–286.
24. J. H. van Dieen, E. P. Westebring-van der Putten, I. Kingma, et al., Low-level activity of the trunk extensor muscles causes electromyographic manifestations of fatigue in absence of decreased oxygenation, *J. Electromyogr. Kines.*, **19**(2009), 398–406.
25. P. V. Komi and C. Bosco, Utilization of stored elastic energy in the leg extensor muscles by men and women, *Med. Sci. Sport Exer.*, **10**(1987), 261–265.
26. M. Ruan and L. Li, Approach run increases preactivation and eccentric phases muscle activity during drop jumps from different drop heights, *J. Electromyogr. Kines.*, **20**(2010), 932–938.
27. Y. Wang and K. Watanabe, Limb dominance related to the variability and symmetry of the vertical ground reaction force and center of pressure, *J. Appl. Biomech.*, **28**(2012), 473–478.
28. S. Prassas and K. Gianikellis, Vaulting mechanics, Applied proceedings of the xxth international symposium on biomechanics in sport—Gymnastics, University of Extremadura, Department of Sport Science, Caceres, Spain, 2002.
29. Z. Y. Kerr, R. Hayden, M. Barr, et al., Epidemiology of national collegiate athletic association women's gymnastics injuries, 2009–2010 through 2013–2014, *J. Athl. Training*, **50**(2015), 870–878.
30. H. Park and D. M. Durand, Motion control of musculoskeletal systems with redundancy, *Biol. Cybern.*, **99**(2008), 503–516.
31. R. E. A. Van Emmerik, J. Hamill and W. J. McDermott, Variability and coordinative function in human gait, *Quest*, **57**(2005), 102–123.
32. E. J. Bradshaw, P. S. Maulder and J. W. Keogh, Biological movement variability during the sprint start: performance enhancement or hindrance? *Sports Biomech.*, **6**(2007), 246–260.